



Surgery in Motion

Intraoperative Laparoscopic Fluorescence Guidance to the Sentinel Lymph Node in Prostate Cancer Patients: Clinical Proof of Concept of an Integrated Functional Imaging Approach Using a Multimodal Tracer

Henk G. van der Poel^{a,*}, Tessa Buckle^{b,1}, Oscar R. Brouwer^{b,1}, Renato A. Valdés Olmos^b, Fijfs W.B. van Leeuwen^{b,*}

^a Department of Urology, Netherlands Cancer Institute – Antoni van Leeuwenhoek Hospital, Amsterdam, The Netherlands

^b Department of Nuclear Medicine, Netherlands Cancer Institute – Antoni van Leeuwenhoek Hospital, Amsterdam, The Netherlands

Article info

Article history:

Accepted March 16, 2011

Published online ahead of print on March 26, 2011

Keywords:

Fluorescence
Image-guided surgery
Sentinel lymph node
SPECT/CT
Prostate cancer

Please visit

www.europeanurology.com and
www.urosources.com to view the
accompanying video.

Abstract

Background: Integration of molecular imaging and in particular intraoperative image guidance is expected to improve the surgical accuracy of laparoscopic lymph node (LN) dissection. **Objective:** To show the applicability of combining preoperative, intraoperative, and postoperative sentinel node imaging using an integrated diagnostic approach based on an imaging agent that is both radioactive and fluorescent.

Design, setting, and participants: Before surgery, multimodal indocyanine green (ICG)-^{99m}Tc-NanoColl was injected into the prostate. Subsequent lymphoscintigraphy and single-photon emission computed tomography/computed tomography (SPECT/CT) imaging of pelvic nodes was performed to determine the location of the sentinel lymph nodes (SLNs) preoperatively. During the surgical procedure a fluorescence laparoscope, optimized for detection in the near infrared range, was used to visualize the nodes identified on SPECT/CT. Eleven patients scheduled for robot-assisted laparoscopic prostatectomy (RALP) with an increased risk of nodal metastasis, based on Memorial Sloan-Kettering Cancer Center/Kattan nomogram estimation, participated in a pilot assessment (N091GF).

Surgical procedure: Patients underwent RALP with LN dissection for prostate cancer.

Measurements: Radioactive and fluorescent signals were monitored using different modalities, and the correlation between the two types of signals was studied. The location of preoperatively detected SLNs was documented.

Results and limitations: Preoperatively, SLNs were identified by SPECT/CT, and the multimodal nature of the imaging agent also enabled intraoperative detection via fluorescence imaging. Fluorescence particularly improved surgical guidance in areas with a high radioactive background signal such as the injection site. Ex vivo analysis revealed a strong correlation between the radioactive and fluorescent content in the excised LNs. Fluorescence detection is limited by the severe tissue attenuation of the signal. Therefore, radio guidance to the areas of interest is still desirable.

Conclusions: Initial data indicate that multimodal ICG-^{99m}Tc-NanoColloid, in combination with a laparoscopic fluorescence laparoscope, can be used to facilitate and optimize dissection of SLNs during RALP procedures.

© 2011 European Association of Urology. Published by Elsevier B.V. All rights reserved.

¹ Authors contributed equally.

* Corresponding authors. Netherlands Cancer Institute, Plesmanlaan 121, 1066 CX Amsterdam, The Netherlands. Tel. +31 205122553; Fax: +31 205122554.

E-mail addresses: h.vd.poel@nki.nl (H.G. van der Poel), fw.v.leeuwen@nki.nl (F.W.B. van Leeuwen).

1. Introduction

Functional (optical) imaging holds great promise to supplement surgeons' eyes and improve surgical outcome [1,2]. One very practical clinical application where imaging can help guide the surgical intervention is the identification of lymph nodes (LNs) draining directly from the tumor (sentinel lymph nodes [SLNs]). Functional imaging of SLNs depends on lymphatic migration and nodal accumulation of the imaging agents [3,4]. Such imaging agents can be relatively simple in design, improving their translational character. For this reason SLN imaging can act as the first clinical precedent for the introduction of new surgical guidance technologies.

The identification of SLNs is common practice in breast cancer and melanoma, for example [5,6]. Although the role of SLN dissection in prostate cancer is still under debate, sentinel lymphadenectomy has been shown to be accurate for LN staging [7,8]. SLNs outside the area of extended pelvic

lymphadenectomy have also been described, underlining the need to document lymphatic drainage pathways for each patient [9]. We reasoned that a more accurate removal of prostate cancer-associated SLNs would help identify the value of nodal resection in prostate cancer patients and might provide better staging. Preoperative single-photon emission computed tomography/computed tomography (SPECT/CT) imaging provides useful anatomic information regarding the location of the SLNs and allows for the identification of SLNs that lie beyond the standard dissection margins [10]. In addition to their diagnostic purposes, these preoperative images can act as a (rough) guide during surgery.

Prostatectomy for cancer has shifted from the open approach toward less invasive laparoscopic and robot-assisted techniques [11]. Although advances in surgical instrumentation have been made, fluorescence-guided (robotic) surgery is still in its infancy. The next step in the technical evolution of surgical interventions is the

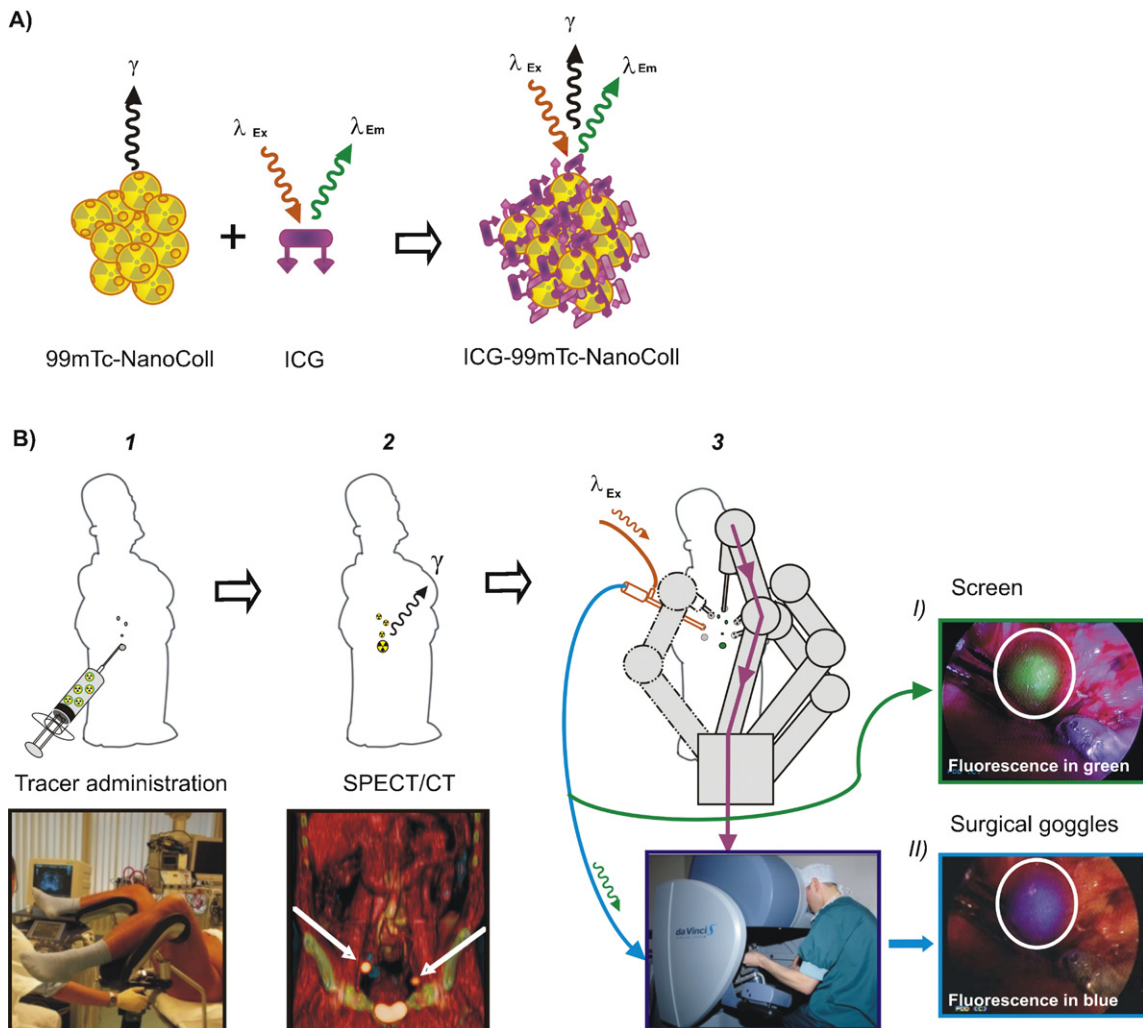


Fig. 1 – Protocol setup. (A) In situ formation of the multimodal radiocolloid that contains both a radioactive and a fluorescent component. (B) (1) Transrectal ultrasound-guided intraprostatic injection of the indocyanine (ICG)-^{99m}Tc-NanoColloid tracer; (2) preoperative single-photon emission computed tomography/computed tomography (SPECT-CT) (arrows indicate sentinel lymph nodes [SLNs]); and (3) intraoperative SLN detection using a near infrared (NIR)-laparoscopic D-light angio NIR fluorescence imaging system (screen I fluorescence depicted in green). The da Vinci S surgical goggles using the system's Tile/Pro function were used to simultaneously depict the three-dimensional surgical field and the intraoperative NIR-laparoscopic image in blue (blue arrow; II). White circles highlight the fluorescent area.

integration of optical imaging modalities that specifically visualize the areas of interest. Most clinical studies regarding optical surgical guidance to the SLNs have focused on the use of a fluorescent imaging agent, for example, indocyanine green (ICG) [12,13]. However, this rapidly migrating imaging agent has to be administered intraoperatively, and its pharmacokinetics and biodistribution cannot be monitored accurately. To circumvent these problems, we developed a hybrid multimodal radiocolloid (ICG-^{99m}Tc-NanoColl; Fig. 1A) that is both radioactive and fluorescent. The principal advantage of this multimodal tracer is that in addition to its optical properties, it retains the well-established functional properties of ^{99m}Tc-NanoColl, including accumulation in the SLNs [14,15].

Here we present the first human studies of an integrated method that enables preoperative planning of the SLN procedure and allows for intraoperative visualization of the SLNs. For this study we used a hybrid radiocolloid that is detectable by gamma camera, SPECT/CT, and near infrared (NIR) fluorescence imaging.

2. Methods and patients

This pilot study applied the concept of a novel multimodal radiocolloid that can be integrated into clinical logistics based on radiocolloids (Fig. 1). The protocol (N091GF, NL28143.031.09) was approved by the local ethics committee of the Netherlands Cancer Institute-Antoni van Leeuwenhoek Hospital. Between June 2010 and January 2011, 11 patients with prostate carcinoma scheduled for robot-assisted laparoscopic prostatectomy (RALP) with an increased risk of nodal metastasis, based on Memorial

Sloan-Kettering Cancer Center/Kattan nomogram estimation, participated in the pilot assessment. The criteria for inclusion were the presence of one or more of the following characteristics: clinical stage >T2b, prostate serum antigen level >10.0 ng/ml, or Gleason sum score >6. Table 1 lists the patient characteristics. The surgical intervention was performed using the da Vinci S robotic system (Intuitive Surgical, USA). During the surgical procedure, both the prostate and SLNs were excised. In addition, in all cases, the nodal areas of the internal, obturator, and external LNs were dissected (retroperitoneal lymph node dissection [RPLND]). LNs proximal to the ureter vessel crossing were only removed when SLNs were detected in this area. All patient studies were performed conform to protocol after written patient consents were obtained.

2.1. Tracer preparation

^{99m}Tc-NanoColl was prepared by adding 1 ml pertechnetate (approximately 700 MBq) in saline to a vial containing NanoColl (GE Healthcare, the Netherlands). After 30 min of incubation at room temperature, ^{99m}Tc-NanoColl formed after the solution was exposed to air via a needle to get rid of any excess reactive elements. ICG-PULSION (Pulsion Medical Systems, Germany) was prepared by dissolving 25 mg of solid ICG in 5 ml of water (suitable for injection).

The ICG-^{99m}Tc-NanoColl injections were prepared by adding 0.050 ml (0.250 mg ICG) of the ICG-PULSION solution to the 1-ml solution of ^{99m}Tc-Nanocoll. The multimodal radiocolloid then formed in situ as reported previously (Fig. 1A) [14–16]. All procedures were performed under good manufacturing practice -z (GMP-z) and kern energie wet (KEW) and with the approval of the local pharmacist.

For diagnostic purposes, ICG can be used intravenously with a dose up to 25 mg/kg; we only used a dose of 0.25 mg for local administration. The ^{99m}Tc-NanoColl was used in a dose (0.5 mg albumin per milliliter of solution) commonly used for SLN imaging of the prostate in our institution [10] without adverse effects.

Table 1 – Patient characteristics in the pilot analysis and ex vivo correlation between the radioactive and fluorescent signal intensities in the excised nodes

	Age, yr	Preoperative PSA (ng/ml)	Prostate size (cm ³)	cT pT	cN pN	cM	cG pG	cG1 pG1	cG2 pG2	SLNs	LNs removed	SLNs with tumor	R ²
1	60	16.3	41	cT2b pT3a	cN0 pN0	cMx	7 7	3 3	4 4	3	8	0	0.97
2	64	8.4	78	cT2c pT2c	cN0 pN0	cMx	7 6	3 3	4 3	0	11	0	0.79/0.97 [§]
3	67	12.2	46	cT2b pT3a	cN0 pN0	cMx	7 8	3 3	4 5	2	11	0	0.91
4	63	16	26	cT2b pT2c	cN0 pN0	cM0	7 9	3 4	4 5	2	13	0	0.98
5	50	4.3	40	cT2b pT2c	cNx pN0	cMx	6 7	3 4	3 3	3	9	0	0.81
6	74	9.8	47	cT2a pT3a	cN0 pN0	cM0	7 7	3 3	4 4	4	10	0	0.99
7	63	27	40	cT2b pT3a	cN0 pN1	cM0	8 10	5 5	3 5	2	6	1	0.91
8	62	24	77	cT2c pT3a	cN0 pN0	cM0	6 6	3 3	3 3	3	16	0	0.71 [*]
9	63	17	35	cT2c pT2c	cN0 pN0	cM0	7 7	3 3	4 4	2	12	0	0.64/0.99 [*]
10 [§]	58	5.1	22	cT3b	cN0	cMx	7	4	3	3	4	2 [§]	0.95
11	62	7.9	23	cT2c pT2c	cN0 pN0	cMx	7 7	3 3	4 3	3	12	0	0.80

PSA = prostate-specific antigen; G = Gleason sum score; c = clinical values; p = pathologic values, respectively; SLN = sentinel lymph node; LN = lymph node; R² = the ex vivo correlation between the fluorescent and radioactive signal intensities.

^{*} One large piece of excised tissue in which the LN was fully surrounded by a thick layer of tissue was omitted in the correlation; the fluorescent signal could not be accurately detected in this specimen.

[§] This patient did not undergo prostatectomy, and due to a lack of lymphatic drainage, no SLN was detected.

[§] Metastases had a tumor size of 0.15 mm and 0.02 mm.

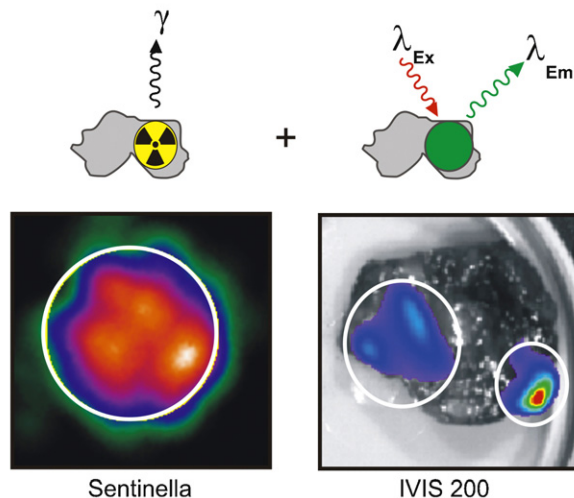
2.2. Tracer administration and imaging

The patients ($n = 11$) were injected in the peripheral zone of the prostate [8] under antibiotic prophylaxis, with ICG- ^{99m}Tc -NanoColl (approximately 280 MBq; 0.4 ml) 3 h before surgery. The ICG- ^{99m}Tc -NanoColl tracer was injected under transrectal ultrasound guidance (Hitachi, Japan) in both lobes of the prostate; each injection was followed by flushing of the needle and tubing with approximately 0.7 ml of saline. A portable gamma camera equipped with a pinhole collimator (Sentinella, OncoVision, Spain) was used to confirm adequate concentration of the tracer in the prostate using its radioactive ^{99m}Tc label. Static planar gamma camera images were acquired at 15 min and 2 h postinjection. These were used to distinguish between sentinel nodes and second echelon nodes as well as to identify unexpected drainage patterns. SPECT/CT (Siemens, Germany) was performed directly after planar imaging at 2 h postinjection. Sentinel nodes were anatomically localized after image fusion. The first node in each nodal basin appearing on early planar imaging was considered the sentinel node. LNs appearing later in the same basin were considered higher echelon nodes. SPECT/CT images were displayed in the operating room to guide laparoscopic detection during RALP.

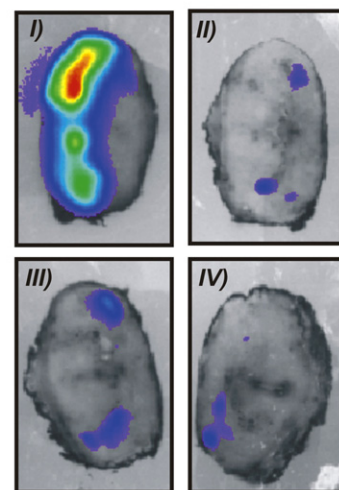
2.3. Surgical technique

After removal of the prostate and ex vivo confirmation of the ICG- ^{99m}Tc -NanoColl presence in the prostate, the SLNs preoperatively localized by SPECT/CT were dissected guided by a laparoscopic gamma probe (Europrobe, London, UK) and the Karl Storz fluorescence laparoscope (Karl Storz, Germany). Both systems were handled by the surgical assistant. In the fluorescence imaging system, 760-nm light, emitted by an internal light source, is guided through a special fluid light cable to a 30 degrees infrared-optimized rigid laparoscope containing an optical filter system. The image was recorded using a charge-coupled device camera. Intraoperative gamma tracing and NIR fluorescence imaging was performed through two 12-mm laparoscopy ports positioned 5 cm lateral to the umbilicus or 2 cm medial from the anterior iliac spine. These are the routinely used assistant ports during RALP and did not interfere with the robotic arms. The fluorescence detection was based on integrated white light and NIR imaging (Fig. 1b3). Via an additional screen attached to the laparoscope, the fluorescent signal was also depicted in green due to a change in the RGB output (Fig. 1b3,I). The laparoscopic image was also projected into the surgeon's goggles (fluorescence in blue) of the da Vinci S using the system's Tile/Pro function (Fig. 1b3, II) during NIR imaging.

A) Signal correlation excised nodes



B) Tracer distribution in the prostate



C) Tracer distribution in four embedded nodes

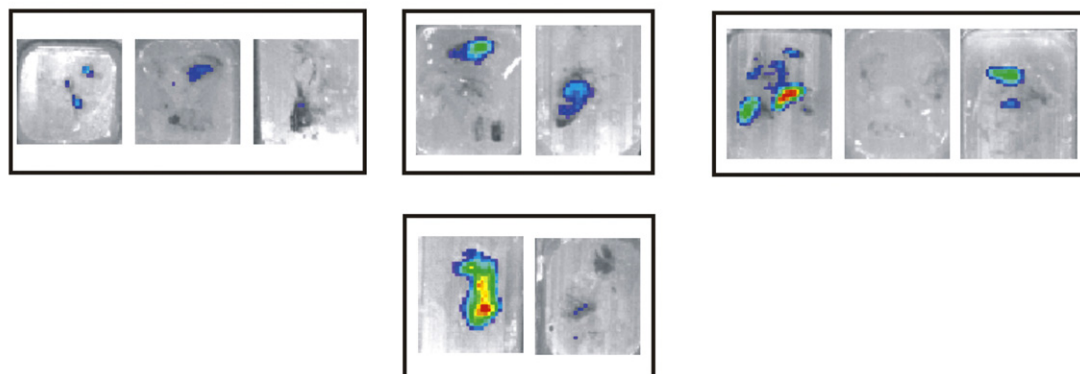


Fig. 2 – Ex vivo analysis. (A) Comparison of indocyanine (ICG)- ^{99m}Tc -NanoColloid signals in an excised tissue specimen that contains lymph nodes. The radioactive signal is detected using the Sentinella gamma camera, and the fluorescent emission was detected using the IVIS 200 fluorescence imager. (B) Fluorescence imaging of the mega-blocks prepared from the excised prostate (order: I–IV) depicts the injection site and the distribution of ICG- ^{99m}Tc -NanoColloid throughout the prostate (measured 3 months after the surgical intervention). (C) Fluorescence analysis also allows detection of the tracer accumulation in embedded (S)SLNs 3 mo after the procedure.

2.4. Ex vivo specimen analysis

Ex vivo examination of the radioactive signal in the excised LNs was performed using a portable gamma camera (Sentinella, Oncovision, Spain; Fig. 2A). The radioactive content of the excised tissue was evaluated by placing the head of the gamma camera at a standardized distance of 10 cm above each excised specimen. Radioactive counts were measured using an acquisition time of 1 min. Signal intensities were quantified using Sentinella Suite (Oncovision) software. Fluorescence signal intensities were measured using an IVIS 200 camera (Xenogen Corp, San Francisco, CA, USA; Fig. 2A). Images were acquired with standard ICG (excitation 710–760 nm and emission 810–875 nm) filter settings. Measured intensities (photons/s/cm²/sr) were quantified using Living Imaging Acquisition and Analysis software (Xenogen Corp, San Francisco, CA, USA). Trendline-based linear regression correlations (determined using Excel) were used to study the correlation between the radioactive and fluorescent signal intensities per patient (Table 1). Fluorescence imaging of paraffin-embedded material was used to visualize the location of the tracer injection and its distribution throughout the prostate (Fig. 2B). Lymphoid tissue specimens were analyzed in a similar manner to evaluate their fluorescent content and the location of the imaging agent in the LNs (Fig. 2C). Unfortunately, our IVIS scanner was not capable of visualizing this distribution on microscale. Trendline-based linear regression correlations (Excel) were used to establish the correlation between the fluorescence intensities and the radioactive count rate findings [16].

3. Results

We have previously shown that using the self-assembled ICG-^{99m}Tc-NanoColl tracer, the lymphatic migration of ICG is positively influenced by the carrier molecule ^{99m}Tc-NanoColl [14–16]. This results in a gradual and specific migration of the tracer from the primary injection site into the draining lymph nodes of the prostate (Fig. 1B; detectable for at least 3–6 h). At 15 min after injection, SLNs were visualized in 55% of the patients. This visualization rate increased to 91% after 2 h. Similar to what has previously reported by Jeschke et al. [17] and Vermeeren et al. [10], it was not possible to detect a SLN in all patients. A total of 27 SLNs were preoperatively detected by SPECT/CT (Table 1); a median number of 2 SLNs (range: 0–4) per patient was found. Important to note is that the preoperative SLN detection method was not influenced by the presence of nodal tumor involvement because in 2 of 11 patients nodal metastases were found (three nodes in total; Table 1), and tumors containing SLNs were not highlighted by the procedure.

During the surgical procedure the SLNs were identified in real time using a combination of a gamma probe and a NIR-optimized fluorescence laparoscope. In the prostatic fossa the background ^{99m}Tc signal from the injection site prevented accurate gamma probe-based navigation to the preoperatively SPECT/CT-defined SLNs. In these cases, however, SLNs could be identified via NIR laparoscopy. In areas where a ^{99m}Tc background signal was less prominent, the fluorescent signal provided guidance during the last centimeter/millimeter of the SLN identification process. The fluorescent signal output of the NIR-optimized fluorescence laparoscope was presented in both blue and green (Fig. 1B). For proper detection of the

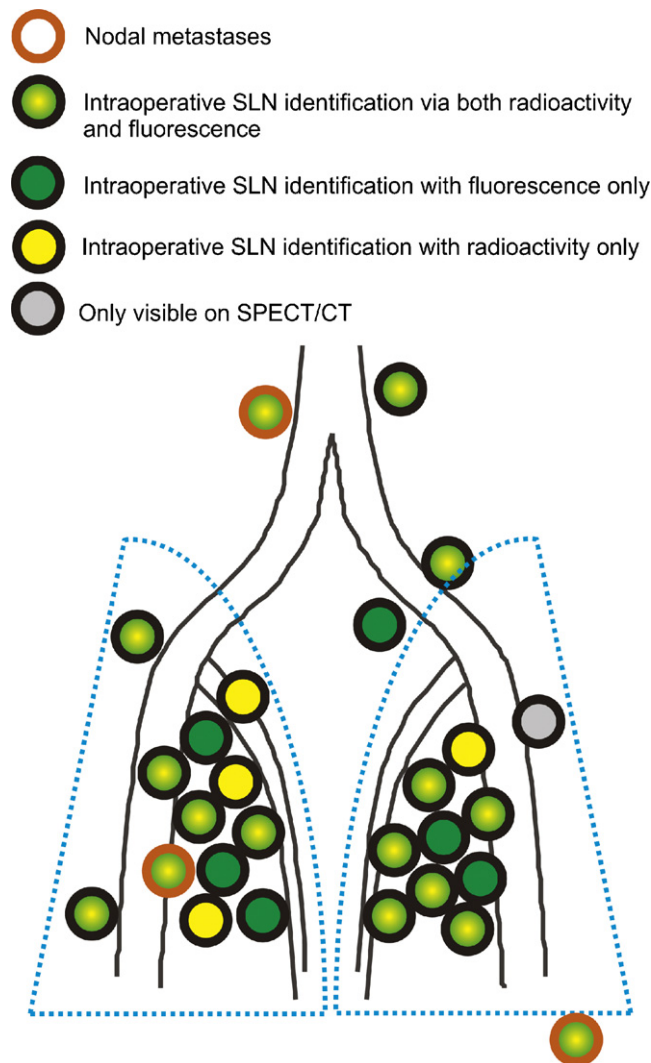


Fig. 3 – Schematic representation of the excised sentinel lymph nodes (SLNs) based on the preoperative single-photon emission computed tomography/computed tomography (SPECT/CT) images, which acts as the gold standard in this scheme, and the modalities with which they could be accurately identified during the surgical procedure. The red circles represent SLNs that contained metastases. The blue dotted lines encompass the extended lymph node (LN) dissection field. Note: The inability to detect some of the SLNs in real time using either the near infrared-optimized laparoscope or the gamma probe is a technical limitation related to the emission type and the modality used because the high R^2 values in Table 1 prove the fluorescent/radioactive signal intensity in all 112 LNs correlates very well.

fluorescent signal, it was required to dim the white-light intensity of the da Vinci system. Generally, overlying tissue (eg, fat, vessels, etc.) obscured the fluorescent image and had to be removed before visualization. One of the 27 preoperatively detected nodes was only detected on SPECT/CT and could not be identified during surgery using either the gamma probe or NIR-optimized laparoscope (Fig. 3). Four of 27 SLNs (15%) could not be detected intraoperatively using the fluorescence laparoscope (Fig. 3). In these cases the LNs were completely embedded in tissue/fat, resulting in a significant attenuation of the fluorescent signal. Overall, no background staining of “free” ICG was observed.

Ex vivo gamma and fluorescence imaging of the dissected nodes (Fig. 2A) showed a high signal intensity correlation for all the individual patient samples ($R^2 \geq 0.71$; total 112 LNs investigated; Table 1). This underlines that all radioactive nodes were indeed fluorescent and to a similar extent. Consequently, visualization difficulties encountered during the surgical procedure (Fig. 3) are not related to the hybrid imaging agent and its migration.

As expected, the improved spatial resolution of fluorescence imaging allows the visualization of the exact location of the ICG- ^{99m}Tc -NanoColl tracer, and as such the (superficial) nodes within the resected tissue specimens (Fig. 2A). Figure 2 also illustrates that ex vivo fluorescence imaging can provide pathologic guidance toward the SLNs embedded in the excised tissue specimens. Three months after the decay of the radioactive signal, the fluorescent signal could still be detected in embedded specimens of the prostate (location of the primary tracer deposits) and lymph nodes (Fig. 2B and 2C).

Finally, the anatomic locations of the by SPECT/CT, intraoperative gamma probe, and/or intraoperative fluorescence imaging identified SLNs were documented (Fig. 3). Five of 27 removed SLNs were located outside the extended dissection field (obturator fossa plus internal iliac plus bifurcation iliac vessels plus common iliac vessels; Fig. 3) [18] and would normally have been missed. In 36% of the patients we found SLNs outside of the extended dissection field, and in two patients these SLNs contained nodal metastases.

4. Discussion

The integrated surgical guidance concept we present here is based on a hybrid imaging tracer (ICG- ^{99m}Tc -NanoColl) that allows for both surgical planning via three-dimensional SPECT/CT and real-time fluorescence-based surgical guidance (Fig. 1B). The radioactive antenna (^{99m}Tc) was used for preoperative imaging and intraoperative guidance to the region of interest. The fluorescent antenna (ICG) is used for improved intraoperative identification of the SLNs.

Migration of ICG- ^{99m}Tc -NanoColl from the injection site was comparable with the migration pattern previously established for ^{99m}Tc -NanoColl, the most frequently used radiocolloid in Europe for SLN procedures in the prostate [8]. This underlines that ICG- ^{99m}Tc -NanoColl retains the functional properties of the original radiocolloid and depicts the uptake in macrophages of the SLN [4]. This behavior is different from blue dyes and “free” ICG, which are rapidly clearing lymphatic perfusion markers. We have previously also shown that NanoColl-based procedures are superior to those based on “free” ICG or ICG bound to (radiolabeled) human serum albumin [16]. In the described procedure any “free” ICG present during injection will thus already have cleared at the time of dissection.

The radioactive component in ICG- ^{99m}Tc -NanoColl enables accurate preoperative assessment of the pharmacokinetics and distribution via lymphoscintigraphy and SPECT/CT. The anatomic information provided by the latter

was shown to improve the SLN detection accuracy up to 98% [10]. During the surgical procedure the SPECT/CT image provides guidance toward the area of the SLN, but the spatial orientation is often related to large anatomic structures such as vessels and bone. Movement of internal anatomy of the patient during the surgical procedure limits the accuracy of sole SPECT/CT-based navigation. Real-time gamma probe detection allows acoustic tracing of the SLN location. This technique, however, suffers from background signals from the injection site (eg, prostatic fossa) and collimator issues that hamper depth perception. The use of ICG- ^{99m}Tc -NanoColl enables us to integrate the advantages of optical fluorescence guidance in these procedures. We found that fluorescence imaging enabled intraoperative identification of the SLNs in the areas where acoustic gamma tracing is inefficient (Fig. 3). In the other areas fluorescence helped identify the exact location of the SLNs with a higher precision.

One of the limitations of fluorescence imaging is the limited tissue penetration of the fluorescent signal, especially through fat and blood. In our study this prevented real-time detection of 15% of the SLNs; only fully exposed nodes could be detected accurately. This limitation of fluorescence imaging also underlines that fluorescence guidance benefits from additional guidance (of the laparoscope) to the regions of interest. Such guidance can be provided by the radioactive component in multimodal imaging agents like ICG- ^{99m}Tc -NanoColl. The next challenge is to investigate if SPECT/CT-based image navigation may help improve the guidance of the tip of the laparoscope to the SLNs [19].

Most clinically used cameras for intraoperative fluorescence guidance are designed for open surgery, for example, photodynamic eye (Hamamatsu Photonics, Hamamatsu City, Japan), the self-built fluorescence-assisted resection and exploration-system [20], and the light-absorption corrected (multispectral) real-time surgical guidance system [21]. Due to the less invasive character of laparoscopic surgery, there is also a clear need to translate the fluorescence guidance technology to laparoscopic surgery. This translation was facilitated by the D-light NIR-optimized fluorescence laparoscope provided by Karl Storz. We found that integration of this laparoscope into the RALP procedures was feasible. The laparoscope could be inserted through one of the existing access ports, and the readout of the fluorescence laparoscope could be integrated into the surgical da Vinci goggles. Limiting in the current setting is that the surgical assistant still has to guide the fluorescence laparoscope manually toward the lesions. Future developments that allow the surgeon independently to guide the tip of the laparoscope toward the lesion via integration in the robotic system are expected to improve the accuracy even further.

In our opinion the widespread development of surgical fluorescence cameras and the development and clinical implementation of new imaging agents are all essential in improving surgical efficacy. Integration of these developments into technical surgical procedures such as minimally invasive robot-guided surgery is crucial. The radioactivity/

fluorescence hybrid approach presented here can easily be expanded into other surgical guidance applications such as tumor bracketing [22] and receptor-targeted tumor imaging [23–25]. Limiting for these extended applications, however, is obtaining approval for the clinical use of new imaging agents. The multimodal ICG-^{99m}Tc-NanoColl imaging agent circumvents this problem because a cocktail of the ICG and ^{99m}Tc-NanoColl, both clinically approved in Europe, is used to form the multimodal complex without the requirement of any chemical modifications or altering the toxicologic profile. As such, ICG-^{99m}Tc-NanoColl facilitates the clinical introduction of the multimodal surgical guidance concept.

5. Conclusions

The hybrid radiocolloid ICG-^{99m}Tc-NanoColl that is both radioactive and fluorescent enabled us to link preoperative SPECT/CT guidance with intraoperative NIR fluorescence laparoscopy. Our initial data also show the feasibility of integrating surgical fluorescence guidance into the RPLND as performed with the da Vinci system. The real-time fluorescence guidance proved particularly valuable in areas where accurate gamma tracing was hindered by background signals.

Author contributions: Henk G. van der Poel and Fijis W.B. van Leeuwen had full access to all the data in the study and take responsibility for the integrity of the data and the accuracy of the data analysis.

Study concept and design: van der Poel, van Leeuwen.

Acquisition of data: van der Poel, Buckle, Brouwer, Valdés Olmos, van Leeuwen.

Analysis and interpretation of data: van der Poel, Buckle, Brouwer, Valdés Olmos, van Leeuwen.

Drafting of the manuscript: van der Poel, Buckle, Brouwer, Valdés Olmos, van Leeuwen.

Critical revision of the manuscript for important intellectual content: van der Poel, Buckle, Brouwer, Valdés Olmos, van Leeuwen.

Statistical analysis: None.

Obtaining funding: van der Poel, van Leeuwen.

Administrative, technical, or material support: Karl Storz endoscopes.

Supervision: van der Poel, Valdés Olmos, van Leeuwen.

Other (specify): None.

Financial disclosures: I certify that all conflicts of interest, including specific financial interests and relationships and affiliations relevant to the subject matter or materials discussed in the manuscript (eg, employment/ affiliation, grants or funding, consultancies, honoraria, stock ownership or options, expert testimony, royalties, or patents filed, received, or pending), are the following: None.

Funding/Support and role of the sponsor: This research was supported, in part, by a KWF translational research award (Grant No. PGF 2009-4344; FvL) and by the Nijbakker Morra stichting. Karl Storz endoscopes supported this research with a D-light system.

Acknowledgment statement: The authors acknowledge the surgical assistants, hospital pharmacy, technical support of the nuclear medicine department, and Michiel Sinaasappel for their contribution and patience. We would also like to acknowledge Hester van Boven and Lenka Vermeeren for their input in setting up this study and Anne van Leeuwen

for her contribution to the clinical approval of the protocol. Rugby club DIOK from Leiden (the Netherlands) is acknowledged for supporting prostate cancer-oriented research via a Movember collection.

Appendix A. Supplementary data

The Surgery in Motion video accompanying this article can be found in the online version at [doi:10.1016/j.eururo.2011.03.024](https://doi.org/10.1016/j.eururo.2011.03.024) and via www.europeanurology.com.

References

- [1] Pleijhuis RG, Graafland M, de Vries J, Bart J, de Jong JS, van Dam GM. Obtaining adequate surgical margins in breast-conserving therapy for patients with early-stage breast cancer: current modalities and future directions. *Ann Surg Oncol* 2009;16:2717–30.
- [2] Keereweer S, Kerrebijn JD, van Driel PB, et al. Optical image-guided surgery—where do we stand. *Mol Imaging Biol* 2010;9:223–31.
- [3] Nunez EGF, Faintuch BL, Teodoro R, et al. Influence of colloid particle profile on sentinel lymph node uptake. *Nucl Med Biol* 2009;36:741–7.
- [4] Faries MB, Bedrosian I, Reynolds C, Nguyen HQ, Alavi A, Czerniecki BJ. Active macromolecule uptake by lymph node antigen-presenting cells: a novel mechanism in determining sentinel lymph node status. *Ann Surg Oncol* 2000;7:98–105.
- [5] Giuliano AE, Kirgan DM, Guenther JM, Morton DL. Lymphatic mapping and sentinel lymphadenectomy for breast cancer. *Ann Surg* 1994;220:391–8.
- [6] Morton DL, Thompson JF, Cochran AJ, et al. Sentinel-node biopsy or nodal observation in melanoma. *N Engl J Med* 2006;355:1307–17.
- [7] Weckermann D, Holl G, Wagner T, Harzmann R. Reliability of preoperative diagnostics and location of lymph node metastases in presumed unilateral prostate cancer. *BJU Int* 2007;99:1036–40.
- [8] Meinhardt W, Valdés Olmos RA, van der Poel HG, Bex A, Horenblas S. Laparoscopic sentinel node dissection for prostate carcinoma: technical and anatomical observations. *BJU Int* 2008;102:714–7.
- [9] Holl G, Dorn R, Wengenmair H, Weckermann D, Sciuk J. Validation of sentinel lymph node dissection in prostate cancer: experience in more than 2,000 patients. *Eur J Nucl Med Mol Imaging* 2009;36:1377–82.
- [10] Vermeeren L, Valdés-Olmos RA, Meinhardt W, et al. Value of SPECT/CT for detection and anatomical localization of sentinel lymph nodes before laparoscopic sentinel node lymphadenectomy in prostate carcinoma. *J Nucl Med* 2009;50:865–70.
- [11] Skolarus TA, Zhang Y, Hollenbeck BK. Robotic surgery in urologic oncology: gathering the evidence. *Expert Rev Pharmacoecon Outcomes Res* 2010;10:421–32.
- [12] Crane LM, Themelis G, Budding T, et al. Multispectral real-time fluorescence imaging for intraoperative detection of the sentinel node in gynecologic oncology. *J Vis Exp* 2010;44, pii 2225.
- [13] Sevic-Muraca EM, Sharma R, Rasmussen JC, et al. Imaging of lymph flow in breast cancer patients after microdose administration of a near-infrared fluorophore. *Radiology* 2008;246:734–41.
- [14] Buckle T, van Leeuwen AC, Chin PT, et al. A self-assembled multimodal complex for combined pre- and intraoperative imaging of the sentinel lymph node. *Nanotechnology* 2010;21:355101.
- [15] Buckle T, Chin PT, van Leeuwen FWB. (Non-targeted) nanosized radioactive/fluorescent imaging agents for combined pre- and intraoperative imaging of the lymphatic system. *Nanotechnology* 2010;21:482001.

- [16] van Leeuwen AC, Buckle T, Vermeeren L, Valdes-Olmos R, van der Poel HG, van Leeuwen FWB. Tracer-cocktail injections for combined pre- and intraoperative multimodal imaging of lymph nodes in a spontaneous mouse prostate tumor model. *J Biomed Opt* 2011;16:016004.
- [17] Jeschke S, Beri A, Grüll M, et al. Laparoscopic radioisotope-guided sentinel lymph node dissection in staging of prostate cancer. *Eur Urol* 2008;53:126–33.
- [18] Briganti A, Blute ML, Eastham JH, et al. Pelvic lymph node dissection in prostate cancer. *Eur Urol* 2009;55:1251–65.
- [19] Ukimura O. Image-guided surgery in minimally invasive urology. *Curr Opin Urol* 2010;20:136–40.
- [20] De Grand GM, Frangioni JV. An operational near-infrared fluorescence imaging system prototype for large animal surgery. *Technol Cancer Res Treat* 2003;2:553–62.
- [21] Themelis G, Yoo JS, Soh KS, Schiltz R, Ntziachristos V. Real-time intraoperative fluorescence imaging system using light-absorption correction. *J Biomed Opt* 2009;14:064012.
- [22] Buckle T, Chin PTK, van den Berg NS, Loo C, Koops W, van Leeuwen FWB. Tumor bracketing and safety margin estimation using multimodal marker seeds; a proof of concept. *J Biomed Opt* 2010;15:056021.
- [23] Kuil J, Velders AH, van Leeuwen FWB. Multimodal tumor-targeting peptides functionalized with both a radio- and a fluorescent-label. *Bioconjugate Chem* 2010;21:1709–19.
- [24] Kuil J, Buckle T, Yuan H, et al. Synthesis and evaluation of a bimodal CXCR4 antagonistic peptide. *Bioconjug Chem* 2011;22:859–64.
- [25] Sampath L, Kwon S, Hall MA, Price RE, Sevick-Muraca EM. Detection of cancer metastases with a dual-labeled near-infrared/positron emission tomography imaging agents. *Transl Oncol* 2010;3:307–17.

Apply for your EAU membership online!

Would you like to receive all the benefits of EAU membership, but have no time for tedious paperwork?

Becoming a member is now fast and easy!

Go to www.uroweb.org and click EAU membership to apply online. It will only take you a couple of minutes to submit your application, the rest - is for you to enjoy!

www.uroweb.org

EAU

**European
Association
of Urology**